



## OPEN

SUBJECT AREAS:  
SUPERCONDUCTING  
PROPERTIES AND  
MATERIALS  
APPLIED PHYSICSReceived  
5 December 2013Accepted  
27 January 2014Published  
11 February 2014Correspondence and  
requests for materials  
should be addressed to  
H.K. (KUMAKURA,  
Hiroaki@nims.go.jp)

# Achievement of practical level critical current densities in $\text{Ba}_{1-x}\text{K}_x\text{Fe}_2\text{As}_2/\text{Ag}$ tapes by conventional cold mechanical deformation

Zhaoshun Gao, Kazumasa Togano, Akiyoshi Matsumoto &amp; Hiroaki Kumakura

National Institute for Materials Science, Tsukuba, Ibaraki 305-0047, Japan.

The recently discovered iron-based superconductors are potential candidates for high-field magnet applications. However, the critical current densities ( $J_c$ ) of iron-based superconducting wires remain far below the level needed for practical applications. Here, we show that the transport  $J_c$  of  $\text{Ba}_{1-x}\text{K}_x\text{Fe}_2\text{As}_2/\text{Ag}$  tapes is significantly enhanced by the combination process of cold flat rolling and uniaxial pressing. At 4.2 K,  $J_c$  exceeds the practical level of  $10^5$  A/cm<sup>2</sup> in magnetic fields up to 6 T. The  $J_c$ - $H$  curve shows extremely small magnetic field dependence and maintains a high value of  $8.6 \times 10^4$  A/cm<sup>2</sup> in 10 T. These are the highest values reported so far for iron-based superconducting wires. Hardness measurements and microstructure investigations reveal that the superior  $J_c$  in our samples is due to the high core density, more textured grains, and a change in the microcrack structure. These results indicate that iron-based superconductors are very promising for high magnetic field applications.

Since the discovery of superconductivity in  $\text{LaFeAsO}_{1-x}\text{F}_x$ , several types of iron-based superconductors have been discovered<sup>1-5</sup>. Among them, K-doped (AE) $\text{Fe}_2\text{As}_2$  (AE = Sr, Ba, 122 type) is most potentially useful for high field applications due to its high critical temperature ( $T_c$ ) value of  $\sim 39$  K, upper critical field ( $H_{c2}$ ) of over 50 T, and relatively small anisotropy<sup>5-8</sup>. Furthermore, the critical angle ( $\theta_c$ ) of the transition from a strong link to a weak link for Ba122 is substantially larger than that for YBCO-based conductors<sup>9</sup>. Recently iron-based coated conductors have been grown by several groups<sup>10-12</sup> utilizing existing YBCO coated conductor technology and have been found to have a self-field  $J_c$  of over 1 MA/cm<sup>2</sup>. Although, at an early stage of development, the transport  $J_c$  in iron-based superconductors reported was disappointingly low due to the weak link grain boundary problem<sup>13-26</sup>, astonishing progress has been made for Ba(Sr)122 wires in the past 3 years.  $J_c$  for Ba(Sr)122 wires approaches  $10^4$  A/cm<sup>2</sup> at 4.2 K and 10 T through metal addition plus rolling induced texture process, hot isostatic press method, cold press method, hot press method and so on<sup>27-36</sup>. These results demonstrated that mechanical deformation is critical for producing high quality superconducting wires, which plays an important role in densifying the conductor core and aligning the grains of the superconducting phase. However, further understanding for process optimization to improve  $J_c$  in Ba(Sr)122 remains limited because we still lack a clear picture about the relationships between processing, microstructure, and superconducting properties. An understanding of the influence of mechanical deformation on the microstructure and superconducting properties will accelerate the development of the appropriate process and will further improve the transport  $J_c$  of Ba(Sr)122 wires. In this work, a comparative study was carried out for pressing and rolling mechanical processes. Variations in grain alignment, core density, microstructure and  $J_c$  in the tapes were systematically investigated. We found that the combined process of cold flat rolling and uniaxial pressing was very useful and effective to achieve practical level  $J_c$  in high magnetic fields.

## Results

The phase impurity and texture of Ba122 tapes were investigated by X-ray diffraction (XRD) analysis of the core surface, from which the silver sheath was mechanically removed. Figure 1 shows XRD patterns of the tapes processed by flat rolling and uniaxial pressing. As a reference, the data for randomly orientated powder is also included in the figure. As can be seen, all samples consist of a main phase,  $\text{Ba}_{1-x}\text{K}_x\text{Fe}_2\text{As}_2$ , however, Ag peaks from the sheath material are also detected. The relative intensities of the (00l) peaks with respect to that of the

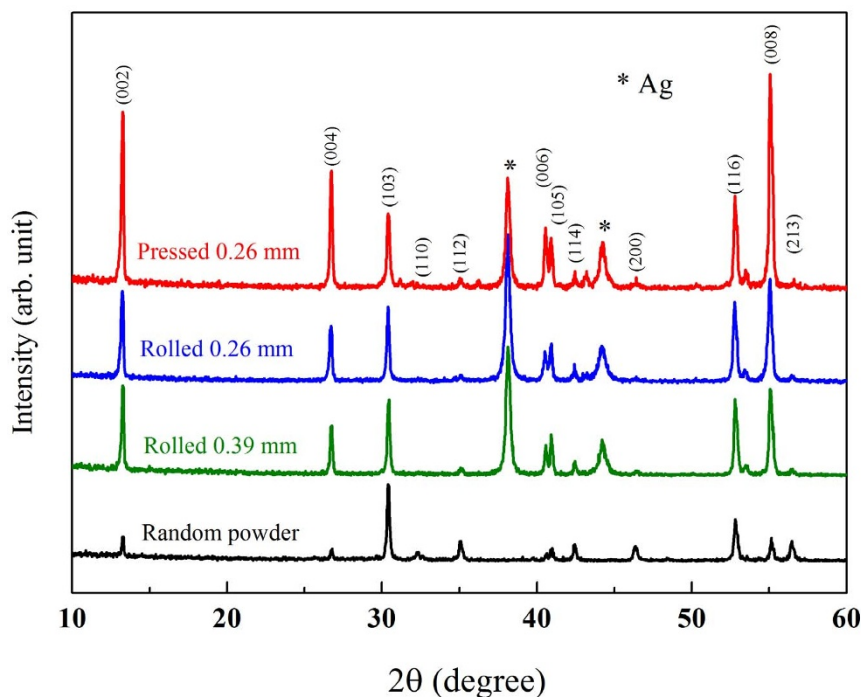


**Figure 1** | X-ray diffraction patterns for  $\text{Ba}_{1-x}\text{K}_x\text{Fe}_2\text{As}_2$  random powder, rolled and pressed tapes fabricated by different deformation processes.

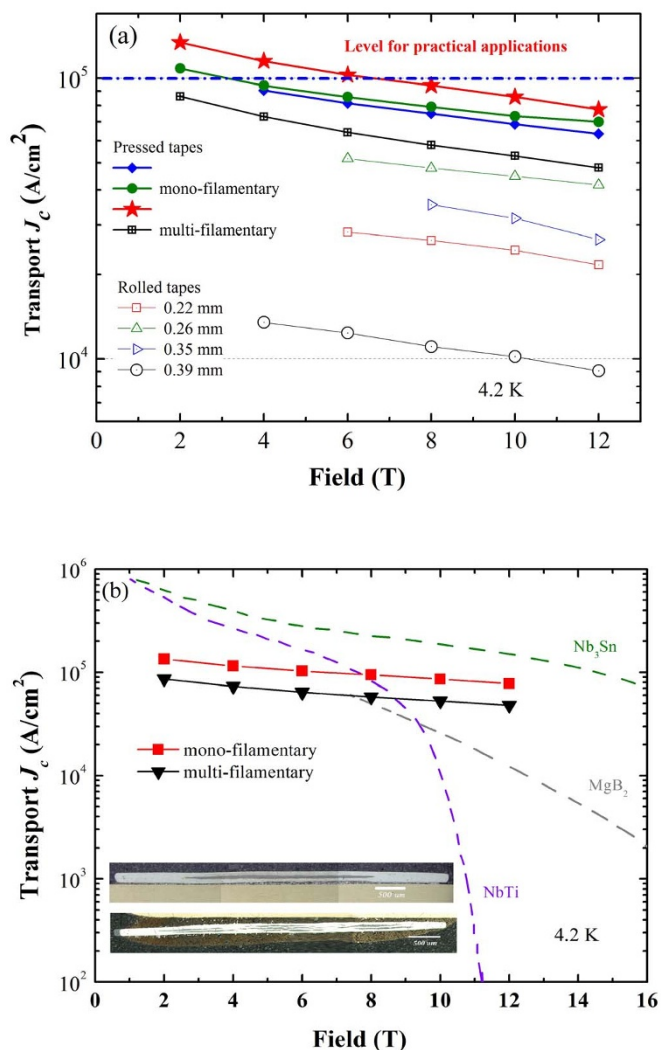
(103) peak in all tape samples, when compared to randomly oriented powder, are strongly enhanced, indicating a well-defined *c*-axis texture. However, it remains at almost the same level within the rolled tapes, suggesting that the grain texture is hardly further improved by the rolling process in our samples. In contrast, stronger relative intensity of (00*l*) peaks was observed in the pressed tape. These results indicate that cold pressing is more effective to improve grain alignment. However, it should be noted that the degree of texture in our pressed tapes is still lower than that in Fe sheathed PIT Sr122 samples<sup>29,31</sup>. This means that the texture could be further enhanced by optimization of processing parameters or by using harder sheath materials.

Figure 2a presents the field dependent transport  $J_c$  of the rolled and pressed tapes. The figure clearly shows that the transport  $J_c$  significantly increases when the rolling thickness is reduced.  $J_c$  achieved a maximum value of  $4.5 \times 10^4$  A/cm<sup>2</sup> at 10 T in the 0.26 mm thick tape. When rolling the tape to smaller thickness, degradation in critical current density was observed. However, further improvement in  $J_c$  values could be achieved for thinner tapes by the application of uniaxial pressing instead of flat rolling. All the pressed tapes show very weak field dependence as observed for the rolled tapes and  $J_c$  well above  $5.0 \times 10^4$  A/cm<sup>2</sup> at 10 T, indicating that a high  $J_c$  is obtained with good reproducibility. It is noteworthy that a high  $J_c$  exceeding the practical level of  $10^5$  A/cm<sup>2</sup> at 4.2 K is obtained in magnetic fields up to 6 T for mono-filamentary tape and  $J_c$  maintains a high value of  $8.6 \times 10^4$  A/cm<sup>2</sup> in 10 T. Even the seven-filamentary tape still sustains  $J_c$  as high as  $5.3 \times 10^4$  A/cm<sup>2</sup> at 10 T. These  $J_c$  values are the highest ever reported for iron-based superconducting wires so far, and they highlight the importance of uniaxial pressing for enhancing the  $J_c$  of iron-based superconductors. Fig. 2b shows the best results for mono and multi-filamentary Ba122 tapes compared to MgB<sub>2</sub>, NbTi and Nb<sub>3</sub>Sn wires. The insets are optical microscope images of cross-sections of the tapes. It can be seen that the  $J_c$  values of the Ba122 tapes exceed the values for MgB<sub>2</sub> and NbTi conductors in magnetic fields higher than 8 T. Furthermore, compared to Nb<sub>3</sub>Sn, the  $J_c$  of Ba122 has a very weak magnetic field dependence and has great potential to surpass the  $J_c$  performance of Nb<sub>3</sub>Sn in

high magnetic fields in the near future. These results indicate that the 122 superconducting wires may be competitive with MgB<sub>2</sub> and the well-established Nb-based conductors for high field generation.

Because of the difficulty of directly measuring the density of the thin superconducting core, researchers usually use Vickers hardness as an indication of the density of the core<sup>37,38</sup>. In this work, we therefore estimated the density of the core from Vickers hardness measurements and investigated the relationships among the core density, the fabrication process, and  $J_c$  values. Fig. 3a displays the influence of flat rolling on hardness and  $J_c$ . This figure gives clear information on layer thickness dependence of  $J_c$ . The  $J_c$  increases with decreasing tape thickness, and reaches a maximum of  $4.5 \times 10^4$  A/cm<sup>2</sup> at 10 T for the 0.26 mm thick tape. As indicated by the XRD measurements, there was almost no difference in grain alignment for the rolled tapes. Therefore, texture can be ruled out as a possible origin of the enhancement of transport  $J_c$ . However, an apparent difference in hardness was observed, the hardness being increased with progress of the rolling process. This indicates that the density might be the main reason for the  $J_c$  enhancement in the rolled tapes. The rapid reduction of hardness and  $J_c$  caused by further rolling to smaller tape thicknesses might be due to microcracks or the sausageing effect. As is known, when the tapes are rolled to very small thicknesses, the working instability becomes a serious problem<sup>39</sup>. In order to further improve  $J_c$ , the technology for rolling to very thin tapes needs to be optimized in the future. Fig. 3b shows the plot of  $J_c$  (10 T, 4.2 K) as a function of hardness for both rolled and pressed tapes. There is a strong linear relation between the hardness of the tapes and  $J_c$ . As the hardness increased, the  $J_c$  of the Ba122 core also increased, however the hardness and  $J_c$  of rolled tapes did not surpass the hardness and  $J_c$  of the pressed tapes respectively. This suggests that uniaxially pressed samples yield much better  $J_c$ -*H* characteristics than the rolled samples<sup>34,35</sup>.

Figure 4 shows typical SEM images of the polished surface for the rolled and pressed tapes. These observations were carried out on the tape plane of the tapes. Although rolling can reduce voids and improve the density of the Ba122 core, the microstructures are still porous and quite inhomogeneous. In contrast, the pressed tapes with



**Figure 2** | (a) Transport  $J_c$  values obtained in this experiment plotted as a function of applied magnetic field. (b) Results for  $J_c$  of mono-filamentary and multi-filamentary Ba122 tapes compared to commercial NbTi, Nb<sub>3</sub>Sn and MgB<sub>2</sub> wires.

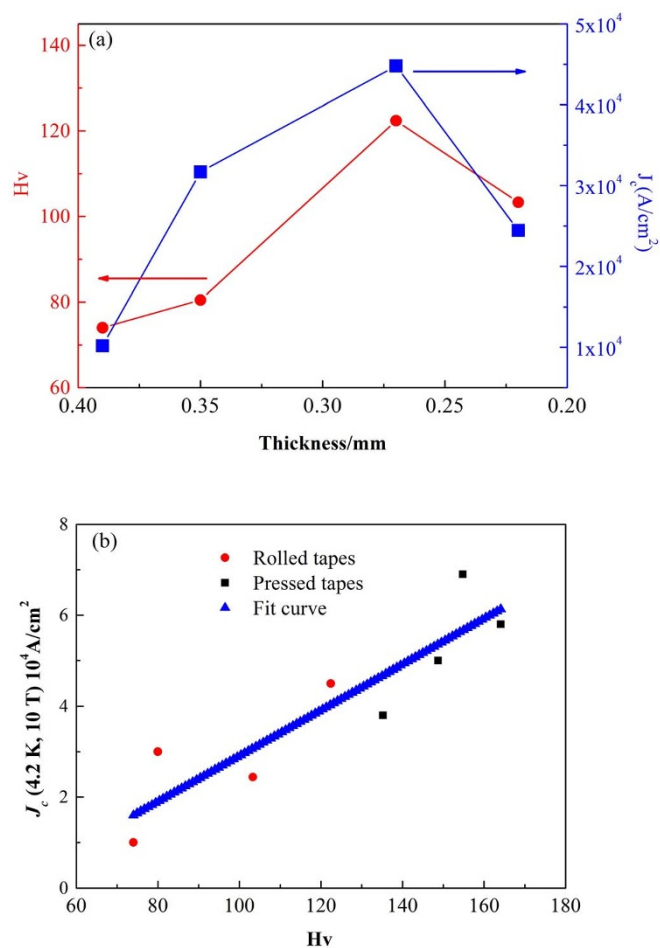


**Figure 3** | (a) The influence of flat rolling on hardness and  $J_c$ . (b)  $J_c$  (10 T, 4.2 K) as a function of hardness for the rolled and pressed tapes.

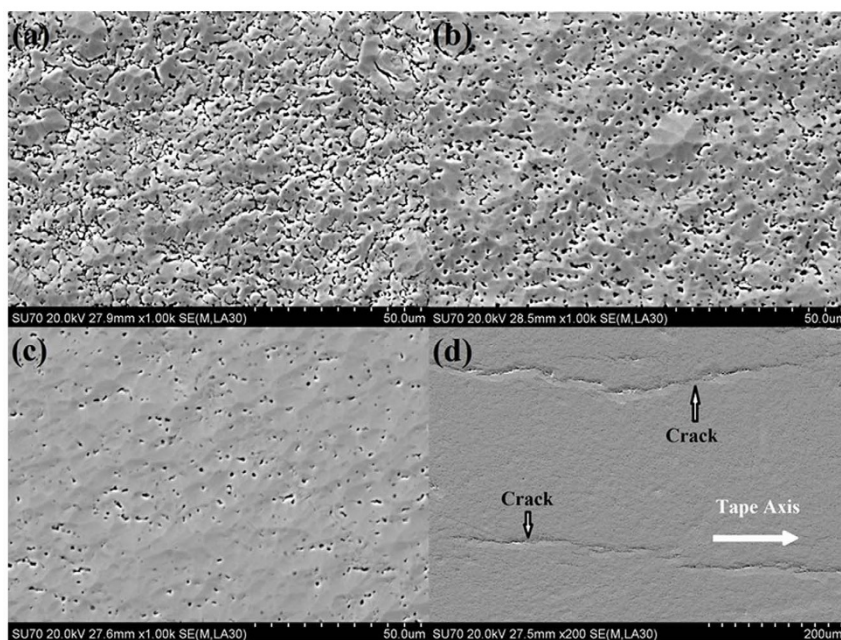


**Figure 4** | SEM surface images of flat-rolled tapes with thickness of 0.39 mm (a) and 0.26 mm (b), and pressed tape (c). The crack structure for the pressed tape (d).





higher hardness and  $J_c$  apparently have a denser and uniform microstructure than the rolled tapes with lower hardness and  $J_c$ . This result is consistent with the hardness analysis. Generally, the force in pressing is larger and more uniform than that in rolling. Thus, the microstructure in the pressed sample is denser and more uniform than that in the rolled one.

## Discussion

Among the many stages of fabrication, flat rolling has been commonly used to densify and align the superconducting core<sup>29,31,40</sup>. Our results showed a large increase in  $J_c$  due to improvement of the core density and preferred orientation in the initial step by the rolling process. Upon further rolling to smaller tape thicknesses, degradation of critical current density was observed. In contrast, when the tape was pressed,  $J_c$  values were significantly increased by further improvement of the core density and grain alignment. Many researchers have previously demonstrated the advantages of pressing for Bi-based tapes<sup>41,42</sup>. This can be attributed to a change in the crack structure<sup>43</sup> and more uniform deformation achieved by pressing rather than rolling. During rolling, pressure varies along the arc of contact between the two rolls and the sample. Stress induced by inhomogeneous pressure in the tape promotes the alignment of cracks transverse to the length direction, thus blocking current flow<sup>35</sup>. However, in the case of uniaxial pressing, the stress direction is rotated 90° with respect to the tape normal resulting in cracks along the direction of the tape length as shown in Fig. 4d. In addition, the forces applied by uniaxial pressing are uniformly distributed perpendicular to the surface of the sample, thus resulting in higher and homogeneous compression. The higher uniform pressure reduces voids, improves texture formation, and thus further improves  $J_c$ . However, it should be emphasized that practical applications of uniaxial pressing for the manufacture of long length wires require specialized machines for continuous pressing of the tape. Fortunately, there have been successful attempts at producing long Ag/Bi-2223 wires by periodic pressing<sup>44</sup> and eccentric rolling<sup>45</sup>, which might be also applied for the production of long length Ba122 wires with high transport  $J_c$ .

Excellent transport  $J_c$  values of  $\sim 10^5$  A/cm<sup>2</sup> under magnetic fields up to 6 T were obtained in uniaxially pressed Ba<sub>1-x</sub>K<sub>x</sub>Fe<sub>2</sub>As<sub>2</sub> tapes. A comparative study of the microstructure and hardness values between pressing and rolling mechanical processes shows that a high core density, more aligned grains and a change in the microcrack structure are responsible for this high  $J_c$  performance in the pressed samples. With further improvements in the critical current density and wire fabrication technology, iron-based superconductors have a very promising future for high-field applications.

## Methods

**Sample preparation.** The precursors of Ba<sub>0.6</sub>K<sub>0.4</sub>Fe<sub>2</sub>As<sub>2.1</sub> were prepared from Ba filings, K plates, Fe powder and As pieces. In order to compensate for loss of elements, the starting mixture contained 10–20% excess K. After ball milling and heat treatment, the precursor was ground into powder using an agate mortar in a glove box filled with high purity argon gas. The powder was packed into an Ag tube (outside diameter: 8 mm, inside diameter: 3.5 mm), which was subsequently groove rolled into a wire with a rectangular cross section of  $\sim 2$  mm  $\times$   $\sim 2$  mm. The wires were deformed into a tape form using a flat rolling machine initially into 0.8 mm in thickness followed by intermediate annealing at 800°C for 2 h and then into 0.40  $\sim$  0.20 mm in thickness. For the pressed samples, the tape was then cut into 35 mm length samples and uniaxially pressed between two hardened steel dies under a pressure of 2  $\sim$  4 G Pa. The rolled and pressed tapes were subjected to a final sintering heat treatment at 850°C for 2  $\sim$  4 h. All heat treatments were carried out by putting the samples into a stainless steel tube, both ends of which were pressed and sealed by arc welding in an Ar atmosphere. We also fabricated seven-filamentary tapes using a similar process. Mono-filamentary wire with diameter of  $\sim 1.3$  mm was cut into seven pieces, bundled together and put into another Ag tube. This assemblage was subjected to deformation, intermediate annealing, and a final heat treatment by the same process as mono-filamentary tape.

**Measurements.** The transport current  $I_c$  at 4.2 K and its magnetic field dependence were evaluated by the standard four-probe method, with a criterion of 1  $\mu$ V/cm. The

transport critical current density,  $J_c$ , was estimated by dividing  $I_c$  by the cross sectional area of the Ba122 core. Magnetic fields up to 12 T were applied parallel to the tape surface. Vickers hardness was measured on the polished cross sections of the tape samples with 0.05 kg load and 10 s duration. For scanning electron microscopy (SEM) observations, we carried out mechanical polishing using emery paper and lapping paper, and then Ar ion polishing using a cross-section polisher, IB-09010CP (JEOL Co., Ltd.), to observe the surface morphology of the tapes precisely using a SU-70 (Hitachi Co., Ltd.).

- Kamihara, Y. *et al.* Iron-based layered superconductor: La[O<sub>1-x</sub>F<sub>x</sub>]FeAs ( $x = 0.05\text{--}0.12$ ) with  $T_c = 26$  K. *J. Am. Chem. Soc.* **130**, 3296–3297 (2008).
- Chen, X. H. *et al.* Superconductivity at 43 K in SmFeAsO<sub>1-x</sub>F<sub>x</sub>. *Nature* **453**, 761–762 (2008).
- Wen, H. H. *et al.* Superconductivity at 25 K in hole-doped (La<sub>1-x</sub>Sr<sub>x</sub>)OFeAs. *Europhys. Lett.* **82**, 17009 (2008).
- Ren, Z. A. *et al.* Superconductivity at 55 K in iron-based F-doped layered quaternary compound Sm[O<sub>1-x</sub>F<sub>x</sub>]FeAs. *Chin. Phys. Lett.* **25**, 2215 (2008).
- Rotter, M., Tegel, M. & Johrendt, D. Superconductivity at 38 K in the iron arsenide Ba<sub>1-x</sub>K<sub>x</sub>Fe<sub>2</sub>As<sub>2</sub>. *Phys. Rev. Lett.* **101**, 107006 (2008).
- Yamamoto, A. *et al.* Small anisotropy, weak thermal fluctuations, and high field superconductivity in Co-doped iron pnictide Ba(Fe<sub>1-x</sub>Co<sub>x</sub>)<sub>2</sub>As<sub>2</sub>. *Appl. Phys. Lett.* **94**, 062511 (2009).
- Putti, M. *et al.* New Fe-based superconductors: Properties relevant for applications. *Supercond. Sci. Technol.* **23**, 034003 (2010).
- Yuan, H. Q. *et al.* Nearly isotropic superconductivity in (Ba, K)Fe<sub>2</sub>As<sub>2</sub>. *Nature* **457**, 565–568 (2009).
- Katase, T. *et al.* Advantageous grain boundaries in iron pnictide superconductors. *Nature Commun.* **2**, 409 (2011).
- Tarantini, C. *et al.* Strong vortex pinning in Co-doped BaFe<sub>2</sub>As<sub>2</sub> single crystal thin films. *Appl. Phys. Lett.* **96**, 142510 (2010).
- Si, W. *et al.* High current superconductivity in FeSe<sub>0.5</sub>Te<sub>0.5</sub>-coated conductors at 30 tesla. *Nature Commun.* **4**, 2337 (2013).
- Trommler, S. *et al.* Architecture, microstructure and  $J_c$  anisotropy of highly oriented biaxially textured Co-doped BaFe<sub>2</sub>As<sub>2</sub> on Fe/IBAD-MgO-buffered metal tapes. *Supercond. Sci. Technol.* **25**, 084019 (2012).
- Yamamoto, A. *et al.* Evidence for electromagnetic granularity in the polycrystalline iron-based superconductor LaO<sub>0.89</sub>F<sub>0.11</sub>FeAs. *Appl. Phys. Lett.* **92**, 252501 (2008).
- Moore, J. D. *et al.* Evidence for supercurrent connectivity in conglomerate particles in NdFeAsO<sub>1-x</sub>. *Supercond. Sci. Technol.* **21**, 092004 (2008).
- Kametani, F. *et al.* Combined microstructural and magneto-optical study of current flow in polycrystalline forms of Nd and Sm Fe-oxypnictides. *Supercond. Sci. Technol.* **22**, 015010 (2009).
- Gao, Z. *et al.* Superconducting properties of granular SmFeAsO<sub>1-x</sub>F<sub>x</sub> wires with  $T_c = 52$  K prepared by the powder-in-tube method. *Supercond. Sci. Technol.* **21**, 112001 (2008).
- Wang, L. *et al.* Structural and critical current properties in polycrystalline SmO<sub>1-x</sub>F<sub>x</sub>FeAs. *Supercond. Sci. Technol.* **22**, 015019 (2009).
- Qi, Y. *et al.* Superconductivity of powder-in-tube Sr<sub>0.6</sub>K<sub>0.4</sub>Fe<sub>2</sub>As<sub>2</sub> wires. *Physica C* **469**, 717 (2009).
- Mizuguchi, Y. *et al.* Fabrication of the iron-based superconducting wire using Fe(Se,Te). *Appl. Phys. Express* **2**, 083004 (2009).
- Lee, S. *et al.* Weak-link behavior of grain boundaries in superconducting Ba(Fe<sub>1-x</sub>Co<sub>x</sub>)<sub>2</sub>As<sub>2</sub> bicrystals. *Appl. Phys. Lett.* **95**, 212505 (2009).
- Ma, Y. *et al.* Fabrication and characterization of iron pnictide wires and bulk materials through the powder-in-tube method. *Physica C* **469**, 651 (2009).
- Wang, L. *et al.* Large transport critical currents of powder-in-tube Sr<sub>0.6</sub>K<sub>0.4</sub>Fe<sub>2</sub>As<sub>2</sub>/Ag superconducting wires and tapes. *Physica C* **470**, 183–186 (2010).
- Wang, L. *et al.* Influence of Pb addition on the superconducting properties of polycrystalline Sr<sub>0.6</sub>K<sub>0.4</sub>Fe<sub>2</sub>As<sub>2</sub>. *Supercond. Sci. Technol.* **23**, 054010 (2010).
- Durrell, J. *et al.* The behavior of grain boundaries in the Fe-based superconductors. *Rep. Prog. Phys.* **74**, 124511 (2011).
- Wang, L. *et al.* Textured Sr<sub>1-x</sub>K<sub>x</sub>Fe<sub>2</sub>As<sub>2</sub> superconducting tapes with high critical current density. *Physica C* **47**, 1689 (2011).
- Fujioka, M. *et al.* Effective Ex-situ Fabrication of F-Doped SmFeAsO Wire for High Transport Critical Current Density. *Appl. Phys. Express* **4**, 063102 (2011).
- Togano, K. *et al.* Large Transport Critical Current Densities of Ag Sheathed (Ba,K)Fe<sub>2</sub>As<sub>2</sub> + Ag Superconducting Wires Fabricated by an Ex-situ Powder-in-Tube Process. *Appl. Phys. Express* **4**, 043101 (2011).
- Togano, K. *et al.* Fabrication and transport properties of ex situ powder-in-tube (PIT) processed (Ba,K)Fe<sub>2</sub>As<sub>2</sub> superconducting wires. *Solid State Communications* **152**, 740 (2012).
- Gao, Z. *et al.* High transport critical current densities in textured Fe-sheathed Sr<sub>1-x</sub>K<sub>x</sub>Fe<sub>2</sub>As<sub>2</sub> + Sn superconducting tapes. *Appl. Phys. Lett.* **99**, 242506 (2011).
- Weiss, J. D. *et al.* High intergrain critical current density in fine-grain (Ba<sub>0.6</sub>K<sub>0.4</sub>)Fe<sub>2</sub>As<sub>2</sub> wires and bulks. *Nature Materials* **11**, 682 (2012).
- Gao, Z. *et al.* High critical current density and low anisotropy in textured Sr<sub>1-x</sub>K<sub>x</sub>Fe<sub>2</sub>As<sub>2</sub> tapes for high field applications. *Sci. Rep.* **2**, 998 (2012).
- Ma, Y. Progress in wire fabrication of iron-based superconductors. *Supercond. Sci. Technol.* **25**, 113001 (2012).



33. Yao, C. *et al.* Microstructure and transport critical current in  $\text{Sr}_{0.6}\text{K}_{0.4}\text{Fe}_2\text{As}_2$  superconducting tapes prepared by cold pressing. *Supercond. Sci. Technol.* **26**, 075003 (2013).
34. Togano, K. *et al.* Enhanced high-field transport critical current densities observed for ex situ PIT processed  $\text{Ag}/(\text{Ba}, \text{K})\text{Fe}_2\text{As}_2$  thin tapes *Supercond. Sci. Technol.* **26**, 065003 (2013).
35. Togano, K. *et al.* Enhancement in transport critical current density of ex situ PIT  $\text{Ag}/(\text{Ba}, \text{K})\text{Fe}_2\text{As}_2$  tapes achieved by applying a combined process of flat rolling and uniaxial pressing. *Supercond. Sci. Technol.* **26**, 115007 (2013).
36. Lin, H. *et al.* Strongly enhanced current densities in  $\text{Sr}_{0.6}\text{K}_{0.4}\text{Fe}_2\text{As}_2$  superconducting tapes. arXiv:1309.7618 [cond-mat.supr-con].
37. Satou, M. *et al.* Densification effect on the microstructure and critical current density in  $(\text{Bi}, \text{Pb})_2\text{Sr}_2\text{Ca}_2\text{Cu}_3\text{O}_x$  Ag sheathed tape. *Appl. Phys. Lett.* **64**, 31 (1994).
38. Parrell, J. *et al.* Direct evidence for residual, preferentially-oriented cracks in rolled and pressed Ag-clad BSCCO-2223 tapes and their effect on the critical current density. *Supercond. Sci. Technol.* **9**, 393 (1996).
39. Osamura, K. *et al.* Work instability and its influence on the critical current density of silver sheathed Bi2223 tapes. *Supercond. Sci. Technol.* **5**, 1 (1992).
40. Flukiger, R. *et al.* Critical currents in Ag sheathed tapes of the 2223-phase in  $(\text{Bi}, \text{Pb})\text{-Sr-Ca-Cu-O}$ . *IEEE Trans. Mag.* **2**, 1258 (1991).
41. Li, Q. *et al.* Critical current density enhancement in Ag-sheathed Bi-2223 superconducting tapes. *Physica C* **217**, 360 (1993).
42. Grasso, G. *et al.* Optimization of the preparation parameters of monofilamentary Bi(2223) tapes and the effect of the rolling pressure on  $J_c$ . *Supercond. Sci. Technol.* **8**, 827 (1995).
43. Korzekwa, D. *et al.* Deformation processing of wires and tapes using the oxide-powder-in-tube method. *Appl. Supercond.* **2**, 261 (1994).
44. Marti, F. *et al.* Progress in critical current density of long Bi(2223) tapes deformed by periodic pressing. *Supercond. Sci. Technol.* **11**, 1251 (1998).
45. Kopera, L. *et al.* New rolling technique for texturing of Bi(2223)/Ag tapes. *Supercond. Sci. Technol.* **11**, 433 (1998).

## Acknowledgments

This work was supported by the Japan Society for the Promotion of Science (JSPS) through its “Funding Program for World-Leading Innovative R&D on Science and Technology (FIRST Program)”. We acknowledge Dr. H. Fujii, Mr. S.J. Ye and Miss Y.C. Zhang of the National Institute for Materials Science for their assistance in  $I_c$  measurements.

## Author contributions

Z.G., K.T. and H.K. designed and conceived the experiments. Z.G. and K.T. carried out the experimental work. A.M. provided the advice and consultation on high magnetic field measurements and microstructure studies. Z.G., K.T. and H.K. contributed to writing the manuscript. H.K. directed the research. All authors discussed the results and implications and commented on the manuscript.

## Additional information

**Competing financial interests:** The authors declare no competing financial interests.

**How to cite this article:** Gao, Z.S., Togano, K., Matsumoto, A. & Kumakura, H. Achievement of practical level critical current densities in  $\text{Ba}_{1-x}\text{K}_x\text{Fe}_2\text{As}_2/\text{Ag}$  tapes by conventional cold mechanical deformation. *Sci. Rep.* **4**, 4065; DOI:10.1038/srep04065 (2014).



This work is licensed under a Creative Commons Attribution-NonCommercial-ShareAlike 3.0 Unported license. To view a copy of this license, visit <http://creativecommons.org/licenses/by-nc-sa/3.0>